

# Extrasolar planet imaging

Antoine Labeyrie\*\* & Hervé Le Coroller  
Collège de France

&

Laboratoire d'Interférométrie Stellaire et Exo-planétaire (LISE)  
Observatoire de Haute Provence  
04870 Saint Michel l'Observatoire, France

## ABSTRACT

The coronagraphic techniques serving to reject most light from a star, when trying to image a nearby planet, can be pushed with an adaptive holographic element. Located after the coronagraph, it can in principle remove most of the residual star light by adding a phase-shifted holographic reconstruction of it. The scheme is also usable within each sub-aperture of a diluted hypertelescope array, sufficiently large to resolve details of an exo-Earth. A possible panoramic version of the previously mentioned Exo-Earth Imager is shaped as a virtual bubble of 400 km diameter, consisting of thousands of 3-meter mirrors, free-flying and arranged co-spherically. The half-size focal sphere is explored by beam combiners, one for each exo-Earth observed within tens of parsecs. Each beam-combiner includes a kilometer-sized corrector of spherical aberration at F/2, which is also diluted and consisting of small free-flyers. The instrument is expected to provide direct coronagraphic images of exo-Earths, resolved in 50x50 resels, with enough dynamic range obtained in 30mn exposures to search colored features and their seasonal variations, indicative of photosynthetic life.

## 1-INTRODUCTION

Coronagraphic techniques proved their worth in the hands of their inventor Bernard Lyot, who obtained the first movies of the solar corona and protuberances. The Lyot coronagraph and its recent variants provide a powerful approach towards imaging exo-planets, but additional forms of cleaning are required to deepen the attenuation of the residual light from the parent star. The methods considered fall in two main classes: 1- incoherent cleaning, applied post detection; 2- coherent cleaning, applied pre-detection.

The first class is more severely limited by the photon statistics. Indeed, the  $N^{1/2}$  fluctuation of detected photons, when  $N$  of them are received in a given speckle, causes a similar RMS residue in the subtracted image. A better nulling, down to one photon per speckle, can be expected with pre-detection subtraction.

NASA recently announced the study and construction of TPF-C, a coronagraphic telescope in space, for obtaining images of exo-Earths at visible wavelengths. It also announced the construction of TPF-1, a long-baseline interferometer using free flyers, for obtaining additional data in the thermal infra-red. The former instrument is an up-dated version, now using a dedicated telescope, of the coronagraphic camera initially proposed to NASA for the Hubble Space Telescope<sup>1</sup>. This precursor coronagraph, built by ESA in the form of the Faint Object Camera, was affected by the spherical aberration of HST's primary mirror, and became inoperant when the COSTAR corrector, added to correct this figuring error, changed the focal ratio.

The original proposal<sup>1</sup> had also involved incoherent cleaning, in the form of rotational image subtraction, to attenuate the stellar residue enough for detecting an exo-Earth image at  $10^{-9}$  intensity relative to the parent star. The telescope rotation procedure was difficult and apparently never attempted. Alternate incoherent methods<sup>2,3,4</sup> have been proposed since.

Coherent cleaning methods were recently and independantly proposed in different forms<sup>5,6,7</sup>. They correct the stellar residue within the coronagraph itself, or downstream with re-imaging stages. This residue is typically speckled if the star is little resolved. I first proposed<sup>5</sup> to uniformize its phase adaptively in the image plane, at the coronagraph exit, and to mask the resulting central peak then appearing in a relayed pupil, before again refocusing the image on the detector. The results of numerical simulations, confirmed by R.Soummer at U.Nice and by R.Lyon at NASA/GSFC, show that this

---

\* labeyrie@obs-hp.fr

attenuates moderately the stellar residue, ten times at best, but larger values can be reached in principle by cascading several such stages.

Codona & Angel<sup>6</sup> proposed to subtract coherently from the residual stellar light a copy of it made with a pair of spatial light modulators. These are illuminated by the main stellar wavefront, usually rejected at the coronagraph entrance, and which they recycle. The subtraction is achieved with a beam splitter and destructive phasing.

This article discusses in more detail another possibility utilizing a hologram in the coronagraph<sup>7</sup>. Beyond the case of monolithic apertures, it also discusses the large hypertelescope interferometers, 100 km or more in aperture size, needed in the longer-term for obtaining resolved images of exo-Earths<sup>8,9</sup>.

## 2. THEORY OF HOLOGRAPHIC NULLING IN A CORONAGRAPH

As previously described, the method uses holographic interferometry to subtract coherently the stellar residue from a copy of it (figure 1). Gabor's classical equations of holography apply to this situation. The hologram is preferably located in the exit pupil of the coronagraph, where is traditionally located the "Lyot stop" diaphragm used for removing the Airy rings. When recording the hologram, the photo-sensitive plate, with coordinates  $u$  and  $v$ , receives complex amplitudes  $O(u,v)$  from the stellar residue, typically speckled, and  $R(u,v)$  from the reference beam, typically a tilted flat wavefront having a uniform and much higher intensity. The hologram is therefore weakly contrasted, and the recorded intensity distribution is :

$$\begin{aligned} I(u,v) &= [R(u,v) + O(u,v)][\overline{R(u,v) + O(u,v)}] \\ &= |R(u,v)|^2 + \overline{R(u,v)}O(u,v) + R(u,v)\overline{O(u,v)} + |O(u,v)|^2 \\ &= |R(u,v)|^2 \left[ 1 + \frac{\overline{R(u,v)}O(u,v)}{|R(u,v)|^2} + \frac{R(u,v)\overline{O(u,v)}}{|R(u,v)|^2} + \frac{|O(u,v)|^2}{|R(u,v)|^2} \right] \end{aligned}$$

where upper lines indicate complex conjugates and vertical bars indicate the modulus. The terms have decreasing moduli since the reference wave is dominant.

The recorded pattern, becoming used as a hologram, has a local intensity transmission:

$\tau_I(u,v) = I(u,v)^\gamma$ , where  $\gamma$  is the classical contrast value of photographic materials. Its amplitude transmission is therefore  $\tau_A(u,v) = I(u,v)^{\gamma/2}$ .

If the hologram is illuminated by the same pair of beams used during the recording exposure, the transmitted complex amplitude is:

$$A_t(u,v) = (R(u,v) + O(u,v))\tau_A(u,v) = [R(u,v) + O(u,v)]I(u,v)^{\gamma/2}$$

Since the first term in the expression of  $I(u,v)$  dominates, a valid approximation for the expansion is:

$$\begin{aligned} A_t(u,v) &\approx [R(u,v) + O(u,v)]|R(u,v)|^\gamma \left[ 1 + \frac{\gamma}{2} \frac{\overline{R(u,v)}O(u,v)}{|R(u,v)|^2} + \frac{\gamma}{2} \frac{R(u,v)\overline{O(u,v)}}{|R(u,v)|^2} + \frac{\gamma}{2} \frac{|O(u,v)|^2}{|R(u,v)|^2} \right] \\ &\approx |R(u,v)|^\gamma \left[ R(u,v) + \frac{\gamma}{2} O(u,v) + O(u,v) + \dots \right] \end{aligned}$$

with additional terms representing various orders diffracted by the carrier grating and becoming separated in the focal plane. The second and third terms are respectively the reconstructed and direct stellar residue. Their sum cancels if  $\gamma = -2$ , thus producing a destructive interference of the stellar residue with its holographic copy.

Physically, this amounts to using a hologram which is recorded on a negative photographic plate, where the carrier grating has dark absorbing lines formed at the location of the bright recorded fringes. When exploited and exposed to the same fringes, the recorded hologram thus blocks the star light. The planet's light is partially transmitted between the dark lines of the hologram.

In classical holography with silver emulsions, recorded holograms were often post-processed with a bleaching chemical, transforming the silver grains into grains of a transparent silver salt, the refractive index of which differs from the gelatin matrix. The phase holograms obtained in this way are also of interest here, and in fact easier to implement, for example in the form of a deformable mirror if the light-sensing function is achieved by a separate component such as a camera, interchanged with the mirror during the cycles of recording and exploitation. .

The planet's wave is mostly transmitted and little affected by the hologram since the comparatively intense reference beam ensures a low diffractive efficiency.

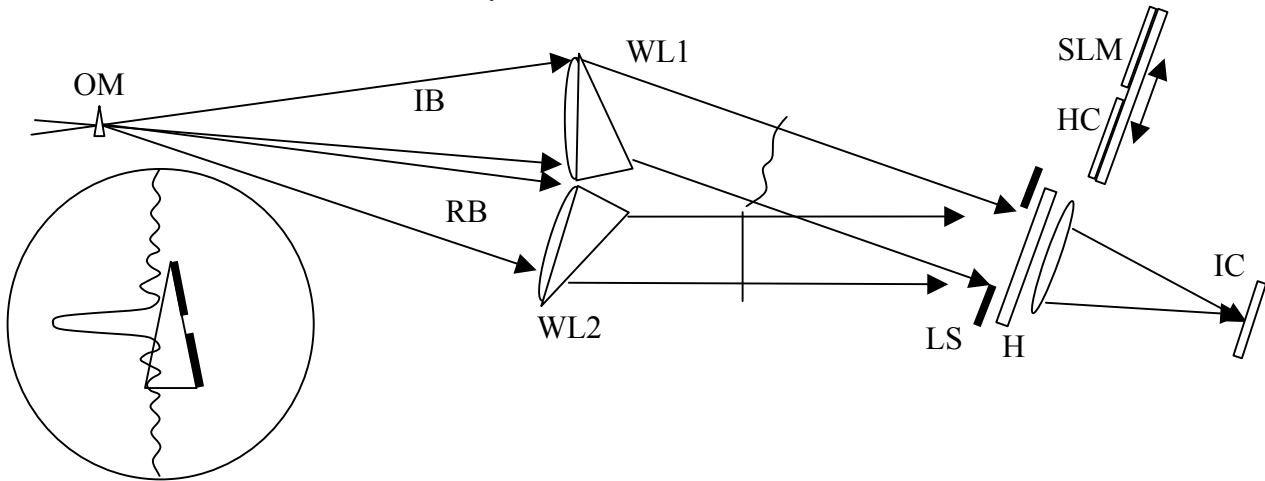


Figure 1: Lyot coronagraph, with a hologram for nulling the residual stellar light. Sketched with dioptric components for clarity, the coronagraph has a focal occulter mask OM in the form of a small optical wedge ( inset), which deviates most stellar light out of the imaging beam IB containing the planet's light. The wedge covers a few rings of the star's Airy spot, according to the usual prescription for Lyot coronagraphy on stars, and also carries a smaller pin-hole for smoothing the far-field pattern of the deviated beam RB. Both beams are collimated and deviated by wedge lenses WL1 and WL2 so as to intersect in the pupil plane, within the aperture of a Lyot stop LS. Being made coherent by adequate spectral filtering, they interfere and produce fringes within the residual stellar speckles of the image beam. The fringes are recorded on a photosensitive plate H, or on a camera HC interchangeable with a spatial light modulator SLM, or deformable mirror, on which the image is displayed. The hologram thus obtained and frozen nulls the residual star light in beam IB by subtracting coherently a reconstructed copy of it. The cleaned image of circumstellar features, including planets, is recorded by camera IC. If, instead of a conventional telescope, the fore optics is a large hypertelescope which resolves the star, the coronagraphic and holographic cleaning must be achieved in each sub-beam separately before combining them to produce the high resolution image. This is achievable with minor changes in the scheme: the mask OM is sized for the large Airy pattern given by each sub-aperture; the Lyot stop LS has multiple holes matching the sub-pupils; and a pupil densifier is added downstream, either before or after the hologram. This hologram is then an array of adjacent holograms, and each is separately optimized in terms of temporal coherence with an array of compensating plates having appropriate thicknesses, inserted after WL2.

### 3.NULLING DEPTH AND THE EFFECT OF PHOTON NOISE

The  $\gamma = -2$  condition ensures in principle a perfect balancing of local amplitudes among the pair of subtracted wavefronts. Nulling residues arise from the neglected terms in the above expressions and from noise in the hologram, including its granularity caused by photon-noise. Regarding this effect of photon noise, a simple calculation<sup>7</sup> indicates that the final stellar residue escaping the holographic nulling amounts, on the average, to one photon per speckle if the hologram recording and observing exposures have the same duration, assuming unit quantum efficiency in the holographic recording material. P.Riaud ( private communication) remarked that the calculation is optimistic since the photons were assumed perfectly aligned along the fringes. Even so, the residual count of stellar photons per speckle is in principle low enough to make planets directly visible if they provide several photons in their image peak.

The nulling can in principle be further improved if the hologram exposure records more photons than the science exposure. This is achievable, without unduely increasing the recording time, by pointing a brighter star or a remote laser

source. A space-based coronagraphic telescope can occasionally aim an artificial star, in the form of a remote laser source, to refresh the hologram, which tends to drift in response to thermal deformations of the telescope optics, its contamination by meteorite dust, etc... . The intense laser light can provide a low-noise hologram in a brief exposure, before repointing the telescope towards the star of interest. In principle, this can further reduce the residual photon count below one photon per speckle.

The pattern of residual star light in any type of coronagraph is known to be highly sensitive to guiding errors. Efficient use of a hologram therefore requires that guiding be achieved with excellent accuracy.

For detecting exo-Earths, the stellar residue should be below  $10^{-9}$ , relative to the intensity of the star's Airy peak in the primary image. This appears achievable in practice with a  $10^{-5}$  coronagraphic residue, not too demanding in terms of primary wavefront errors, and a further  $10^{-4}$  nulling gain achieved by the hologram.

#### **4. PRACTICAL IMPLEMENTATION**

Several types of holograms may be considered. The classical holographic plates based on silver halide emulsions have a modest quantum efficiency, use slow chemical processing, and cannot easily be used repeatedly. Recent holographic materials such as certain photopolymers are better in most respects, but the molecular scale of their light response makes them very little sensitive. Opto-electronic devices behaving like phase holograms can also be made in the form of a deformable mirror, such as used for adaptive optics, displaying the image detected by a camera. MEMS-based versions, such as marketed by Boston Micromachines, are already available with 32x32 actuators and moderate noise. Liquid-crystal versions, called "spatial light modulators" or SLMs are commercially available with 512x512 pixels but require polarized light. Such opto-electronic holograms, where the recording and diffraction functions are achieved by separate components, are conveniently recordable and erasable as needed. Their detective quantum efficiency, defined by the recording camera, can be nearly photon-limited with the recent CCD's incorporating on-chip electron multiplication (EEV-Marconi, Texas Inst), although tube intensifiers apparently remain better, at the expense of a lower quantum efficiency. Because the camera and active diffractive element are separate components, a moving carriage is needed to interchange the camera and hologram for the hologram exposure and science cycles. A beam splitter can replace it if the light loss is tolerable (if a laser star is used, a ultra-narrow-band dichroic mirror can be used for minimal loss of starlight) . The optimal cycling period to be adopted, milliseconds on Earth and up to hours in space, is defined by the lifetime of the residual stellar pattern.

#### **5. ACHROMATIZATION**

The pattern of residual stellar light, typically speckled in the image and the pupil plane, and the hologram obtained by adding the reference wave, are both chromatic. This restricts severely the usable spectral bandwidth, unless suitable precautions are taken. There are several possible approaches:

- 1- spectrally splitting the beam into a series of adjacent spectral channels, each equipped with a holographic nuller;
- 2- if the hologram is located in the exit pupil of the coronagraph, as shown in fig. 1, it can be approximately achromatized by dispersing the reference beam. It can indeed be shown that the speckled pattern of residual starlight in the exit pupil is nearly wavelength-invariant if the wavefront from the telescope aperture has weak bumpiness and a uniform modulus.
- 3- using a thick hologram and exploiting the wavelength selectivity of its Bragg reflection to record independent holograms at different wavelengths in a single component .

#### **6. CASE OF HYPERTELESCOPES AND THE EXO-EARTH IMAGER**

Diluted optical arrays used with a densified exit pupil, i.e. in the hypertelescope mode of direct imaging<sup>8</sup>, can feed a coronagraph. The exit pupil of the hypertelescope can be completely filled, for example if the entrance aperture is a square or hexagonal array of sub-apertures in the entrance aperture. Such filled exit pupils are particularly efficient for most coronagraphic designs. In particular, the central obscuration and spider supports, which often degrade the

coronagraphic performance of telescopes, are easily avoided in hypertelescopes by off-setting the focal station in such a way that its shadow falls between the primary apertures.

Once adjusted, with all optical paths balanced within Rayleigh's tolerance, a hypertelescope having such a dense exit pupil can be exploited for coronagraphy like a conventional telescope. The residual wavefront errors can be classified as tip-tilt and piston errors at the primary mirrors, plus those arising from the figure errors within each such mirror. In the coronagraphic output image, piston errors tend to dominate in terms of their contribution to the speckled stellar halo.

The hologram method is applicable to null the residual stellar light, provided that the star is unresolved by the large aperture. The condition is typically met for an infra-red hypertelescope, operating at 10 microns, with baselines extending over a few hundred meters to separate the planet from the star. At visible wavelengths the same instrument typically resolves the star's apparent disk, and the hologram method is then unsuitable if applied to the combined image. However, it can be applied before combining the sub-images, that is within each sub-aperture.

Such pre-combiner coronagraphy is also obviously needed in the extreme case of an Exo-Earth Imager. As shown through simulations<sup>9</sup>, obtaining resolved snapshot images of an exo-Earth at 10 parsecs requires a non-redundant array of 100 or more apertures, 3 meter in size if the exposure is to last less than 30mn to avoid blurring by the planet's rotation. The parent star is highly resolved in such conditions, and should therefore be nulled as deeply as possible before combining the sub-images. The basic hologram arrangement sketched in figure 1 can be adapted to this situation, as explained in the figure caption.

Concepts for the Exo-Earth Imager have been discussed previously<sup>8,9</sup>. The spherical version shown in figure 2 has static primary elements, each of which can feed several focal combiners.

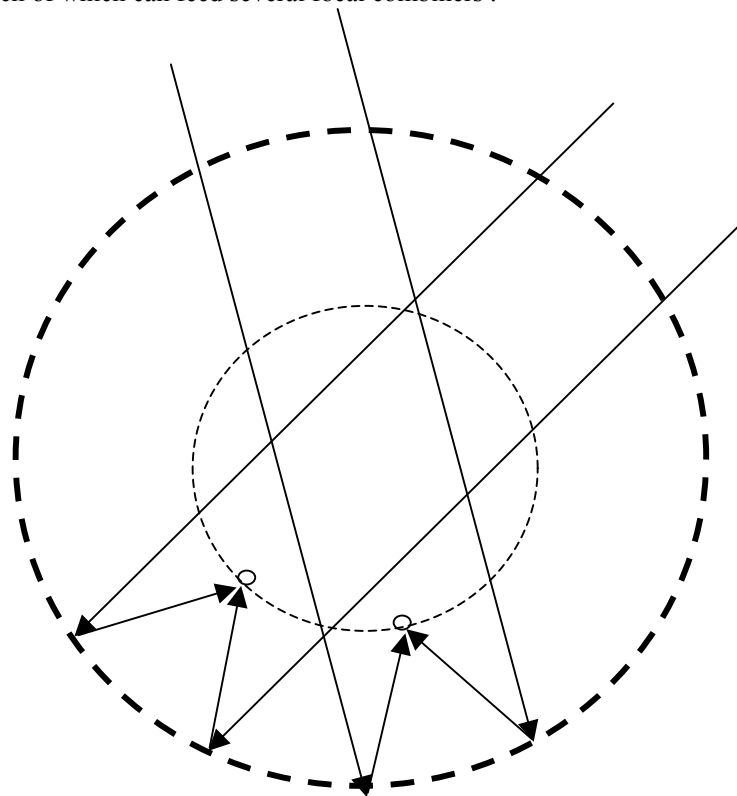


Figure 2 : spherical version of the Exo-Earth Imager, with 10,000 mirrors of 3-meter size forming the diluted primary sphere. For 100-kilometer effective apertures, the sphere's diameter is 800 km. 1-kilometer flotillas of small secondary mirrors are located near the half-size focal sphere and correct the spherical aberration. These can be arranged like a clam-shell corrector, in diluted form, to also correct the coma. Pointing is achieved by moving these focal free-flyers. The primary elements are static. Small rigid solar sails suffice to maintain their configuration at sites such as L2. Accurate metrology is achievable with a laser interferometer aiming the primary and secondary elements from the sphere's center.

A tempting way of searching for exo-life on resolved exo-Earth images, such as those obtainable with a large Exo-Earth Imager hypertelescope, involves the discrimination of colored patches having a non-mineral origin. Minerals such as opals and other photonic crystals can have reflectance spectra with virtually any profile, possibly resembling those of photosynthetic organisms. Conceivably, spectra of minerals can even be temperature dependant, and hence influenced by diurnal and seasonal cycles. Photo-synthetic life, instead, also responds to the quantum effect of light, and not just the thermal effect. This explains why the springtime greening on Earth, in the temperate zone, begins before the local soil and air begin to heat. Thermal inertia thus delays the temperature cycle with respect to the insolation cycle, and greening is much influenced by the latter. Such effects are potentially observable on exo-Earths with large hypertelescopes having holographic coronagraphs in their sub-pupils. Together with other spectro-imaging cues, they can provide a robust discrimination of life.

## 6. NUMERICAL AND LABORATORY SIMULATIONS INITIATED

Numerical simulations are undertaken by one of us (HLC). The preliminary result shown in figure 3 does not yet incorporate photon noise, and therefore assumes a low-noise hologram such as obtainable with a laser star. It shows the effect of the neglected terms in the above equations, which generate weak side-lobes in the planet's field and may in some cases limit the nulling depth achievable. This contamination appears to be very weak but its impact will have to be assessed in more detail. Also, the hologram can relax the bumpiness tolerances at the primary wavefront, and simulations are expected to indicate the optimal specifications.

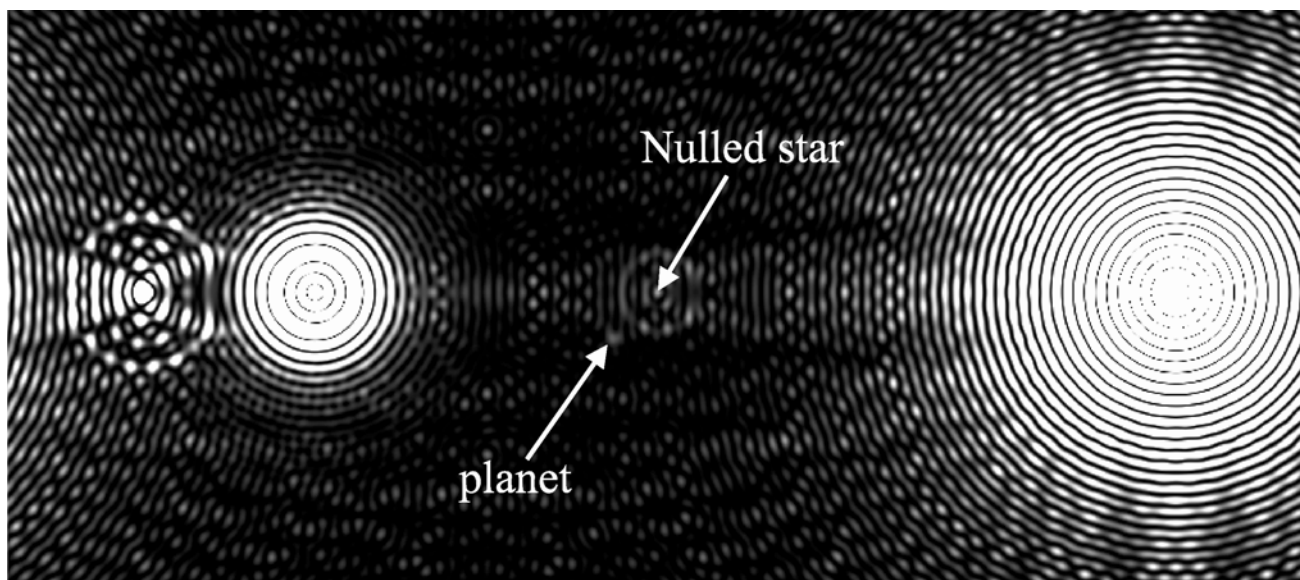


Figure 3: Preliminary numerical simulation of an exo-planet image in a Lyot coronagraph with a hologram nulling the residue. The planet's relative intensity is  $10^{-6}$  in this example. The bright patterns at left and right are diffracted orders of the hologram carrier grating.

Laboratory simulations are also initiated by F.Martinache. These initially utilize photopolymers as holographic materials. The hologram is a form of adaptive element which is comparatively simple to use in such simulations.

## 7. CONCLUSIONS AND FUTURE WORK

The coherent cleaning of coronagraphic residues can in principle enhance markedly the detection of weak circumstellar objects such as exo-planets. Its holographic form uses a hologram or synthetic hologram as the adaptive

correcting element. It can in principle null the stellar residue below a few photons per speckle, and even less if the hologram is recorded with a laser star. The principle is also applicable to large hypertelescopes for resolving details of exo-Earths, in which case a separate coronagraph and hologram are needed in each sub-pupil. This provides a path towards detecting exo-life. Following some preliminary numerical simulations, laboratory simulations are under way.

#### REFERENCES

1. A.Bonneau, M.Josse & A.Labeyrie , *Image Processing Techniques in Astronomy*, **54**,403-409, 1975 ( **posted at : [www.oamp.fr/lise/ biblio.html](http://www.oamp.fr/lise/biblio.html)**)
2. KenKnight C., "Methods of detecting extrasolar planets".I Imaging, *Icarus*, 30,422 1977.
3. A.Labeyrie,, *A&A* **298**, 544-546, 1995
4. O.Guyon, in print 2004
5. A.Labeyrie proc. ITHD 2002 school, Nice, EAS Pub. Series , ( C. Aime & R.Soummer, editors.),
6. J.L.Codona & R.Angel, *Ap.J.*,**604,2**, 2004
7. A.Labeyrie, proc. ITHD school, Nice 2003, EAS Pub. Series, ( C. Aime & R.Soummer, editors.), in print.
8. A.Labeyrie, *A&A*, Supp. Series, **118**, 517-524, 1996
9. A.Labeyrie, *Science*, Sep. 17, 1864-1865, 1999